

# Phase transitions of a single polyelectrolyte in a poor solvent with explicit counterions

Anoop Varghese,<sup>\*</sup> Satyavani Vemparala,<sup>†</sup> and R. Rajesh<sup>‡</sup>

*The Institute of Mathematical Sciences, C.I.T. Campus, Taramani, Chennai 600113, India*

(Dated: February 18, 2022)

## Abstract

Conformational properties of a single flexible polyelectrolyte chain in a poor solvent are studied using constant temperature molecular dynamics simulation. The effects of counterions are explicitly taken in to account. Structural properties of various phases and the transition between these phases are studied by tracking the values of asphericity, radius of gyration, fraction of condensed counterions, number of non-bonded neighbours and Coulomb interaction energies. From our simulations, we find strong evidence for a first-order phase transition from extended to collapsed phase consistent with earlier theoretical predictions. We also identify a continuous phase transition associated with the condensation of counterions and estimate the critical exponents associated with the transition. Finally, we argue that previous suggestions of existence of an independent intermediate phase between extended and collapsed phases is only a finite size effect.

PACS numbers: 82.35.Rs, 36.20.Ey, 64.70.km

## I. INTRODUCTION

Polyelectrolytes are polymers, which in a polar solvent, release counterions into the solution, making the polymer backbone charged. Examples of polyelectrolytes include sulfonated polystyrene, polymethacrylic acid, DNA, RNA and proteins. Though the system is overall charge neutral, long range Coulomb interactions make the behaviour of polyelectrolytes considerably different from that of neutral polymers [1, 2]. The static and dynamic properties of polyelectrolytes depend on the nature of the solvent, linear charge density of the polymer backbone, valency of the counterions, temperature, salt concentration, hydrodynamic interactions and the bending rigidity [1, 3].

A polyelectrolyte chain in a poor solvent undergoes a series of phase transitions as the linear charge density of the chain is varied keeping temperature fixed. The rich phase diagram resulting from a competition between the long range Coulomb interaction and the short range excluded volume interaction has been studied theoretically [4–11], numerically [6–8, 12–15] and experimentally [16–22]. At very low charge densities, the polyelectrolyte chain is in a collapsed phase, with the counterions uniformly distributed throughout the solution [15]. On increasing the charge density, the polyelectrolyte chain makes a transition into the pearl-necklace phase in which the chain has two (dumbbell) or more globules connected through a string of monomers [4–7]. This instability of the charged collapsed phase is similar to the Rayleigh instability of a charged droplet [23, 24]. While the pearl-necklace phase has been observed in numerical simulations [14, 15, 25], the experimental status is unclear [16, 19, 21]. Further increase in charge density decreases the number and size of the globules and the

polyelectrolyte chain becomes extended. When the linear charge density exceeds a threshold value, the electrostatic energy dominates over the thermal fluctuations and the counterions condense on the polyelectrolyte chain [9]. The condensed counterions form dipoles with the polymer monomers and the attraction among the dipoles leads to the collapse of the polyelectrolyte chain [12]. Recent simulations also show that, in extreme poor solvent conditions, the polyelectrolyte chain can make a direct transition from the initial collapsed phase to the final condensed collapsed phase without encountering some or even all the intermediate phases [15].

Certain features of the phase diagram remain poorly understood. Recent simulations argue for the existence of an intermediate phase between the extended and the condensed collapsed phases [14, 15]. Referred to as the sausage phase, this phase is defined as a collapsed phase in which the shape of the collapsed polymer becomes aspherical, having a non-zero mean asphericity. It is not clear whether this phase is just a finite size effect.

In addition, the nature of the counterion condensation is not well understood. By studying the condensation of counterions on a cylinder in three dimensions, and on a disc in two dimensions, it was shown that condensation is a second order phase transition [26–28]. However, to the best of our knowledge, the corresponding question has not been addressed for a three dimensional polyelectrolyte chain system.

In this paper, we simulate polyelectrolyte chains of different lengths and varying charge densities. We argue that the sausage phase does not exist and is an artefact of studying very small chains. Our simulations also show strong evidence that the counterion condensation is a second order transition accompanied by a divergence in the fluctuations of the number of non-bonded nearest neighbours of a monomer. In addition, we study aspects of the extended to collapsed transition.

<sup>\*</sup>Electronic address: anoop@imsc.res.in

<sup>†</sup>Electronic address: vani@imsc.res.in

<sup>‡</sup>Electronic address: rrajesh@imsc.res.in

## II. MODEL AND SIMULATION METHOD

We model the polyelectrolyte chain as spherical beads (monomers) connected through springs where each monomer carries a charge  $qe$ . Counterions are monovalent and are modelled as spherical beads, each carrying a charge  $-qe$ . The polyelectrolyte chain and the counterions are assumed to be in a medium of uniform dielectric constant  $\epsilon$ . The potential energy due to the pair of particles  $i$  and  $j$  consists of three interactions.

**Coulomb interaction:** The electrostatic energy is given by

$$U_c(r_{ij}) = \frac{Zq^2e^2}{4\pi\epsilon r_{ij}}, \quad (1)$$

where  $Z = -1$  for monomer-counterion pairs and  $Z = 1$  otherwise, and  $r_{ij}$  is the distance between particle  $i$  and  $j$ .

**Excluded volume interaction:** The excluded volume interactions are modelled by the Lennard-Jones potential, which for two particles at a distance  $r_{ij}$ , is given by

$$U_{LJ}(r_{ij}) = 4\epsilon_{ij} \left[ \left( \frac{\sigma}{r_{ij}} \right)^{12} - \left( \frac{\sigma}{r_{ij}} \right)^6 \right], \quad (2)$$

where  $\epsilon_{ij}$  is the minimum of the potential and  $\sigma$  is the inter particle distance at which the potential becomes zero. We use reduced units, in which the energy and length scales are specified in units of  $\epsilon_{ij}$  (counterion-counterion) and  $\sigma$  respectively. The depth of the attractive potential  $\epsilon_{ij}$  is chosen as 1.0 for monomer-counterion and counterion-counterion pairs and 2.0 for monomer pairs, while  $\sigma$  is set to 1.0 for all pairs. We use the shifted Lennard-Jones potential in which  $U_{LJ}(r_{ij})$  is set to zero beyond a cut off distance  $r_c$ . The value of  $r_c$  equals 1.0 for monomer-counterion and counterion-counterion pairs and 2.5 for monomer-monomer pairs. With this choice of the parameters, the excluded volume interaction is purely repulsive for all the pairs other than the monomer-monomer pairs. The effective short range attraction among the monomers mimics poor solvent conditions. Other ways of realising poor solvent conditions may be found in Ref. [25].

**Bond stretching interaction:** The bond stretching energy for pairs in the polymer that are connected directly through springs is given by

$$U_{bond}(r_{ij}) = \frac{1}{2}k(r_{ij} - b)^2, \quad (3)$$

where  $k$  is the spring constant and  $b$  is the equilibrium bond length. The values of  $k$  and  $b$  are taken as 500 and 1.12 respectively. This value of  $b$  is close to the minimum of Lennard-Jones potential.

The relative strength of the electrostatic interaction is parametrised by a dimensionless quantity  $A$ :

$$A = \frac{q^2\ell_B}{b}, \quad (4)$$

where  $\ell_B$  is the Bjerrum length [29], the length scale below which electrostatic interaction dominates thermal fluctuations.

$$\ell_B = \frac{e^2}{4\pi\epsilon k_B T}, \quad (5)$$

where  $k_B$  is the Boltzmann constant and  $T$  is temperature. The thermal fluctuations dominate over the electrostatic interactions for very low values of  $A$  and the counterions will be uniformly distributed in the solution. When  $A$  is of order one, the electrostatic interaction energy is comparable to the thermal energy and the counterions begin to undergo Manning condensation[9]. In our simulation, we vary  $A$  from 0.055 to 14.29.

The equations of motion are integrated in time using the molecular dynamics simulation package LAMMPS [30, 31]. The simulations are carried out at constant temperature ( $T=1.0$ ), maintained through a Nosé-Hoover thermostat (coupling constant = 0.1) [32, 33]. The system is placed in a cubic box with periodic boundary conditions. At the start of the simulations, the configuration of the chain is randomly chosen and the monovalent counterions are distributed uniformly throughout the volume such that the charge neutrality is achieved. In our simulations, the length  $N$  of the chain is varied from 50 to 400, keeping the overall particle density of the system fixed at a constant value,  $7.23 \times 10^{-6}$  particles per  $\sigma^3$ . At this density, there is no direct contact between the polyelectrolyte chain and any of its periodic images. We use the particle-particle/particle-mesh (PPPM) technique [34] to evaluate the energy and forces due to the long range Coulomb interactions. The time step of the integration is chosen as 0.001. Our simulation runs are divided into an equilibration run ( $5 \times 10^6$  steps), followed by a production run ( $6 \times 10^6$  steps). All the data shown in the plots are measurements over only the production run ( $1.2 \times 10^5$  configurations). The errors in the plots are estimated by dividing the production into five statistically independent blocks and measuring the standard deviation of the mean values of the observable in each block [35].

## III. RESULTS AND DISCUSSION

### A. Configurations of the polyelectrolyte chain

Snap shots of the polyelectrolyte configuration for different values of  $A$  are shown in Fig. 1. For very small values of  $A$ , the electrostatic interactions can be ignored, and the polymer exists in a collapsed phase [Fig. 1(a)]. As  $A$  is increased, the globule breaks up into two [Fig. 1(b)] or more smaller globules [Fig. 1(c)]. This pearl-necklace configuration becomes extended on further increasing  $A$  [Fig. 1(d)]. Counterion condensation is initiated and for sufficiently large  $A$ , the polymer undergoes a collapse transition to form a sausage phase [15] [Fig. 1(e)] or a spherical globule [Fig. 1(f)].

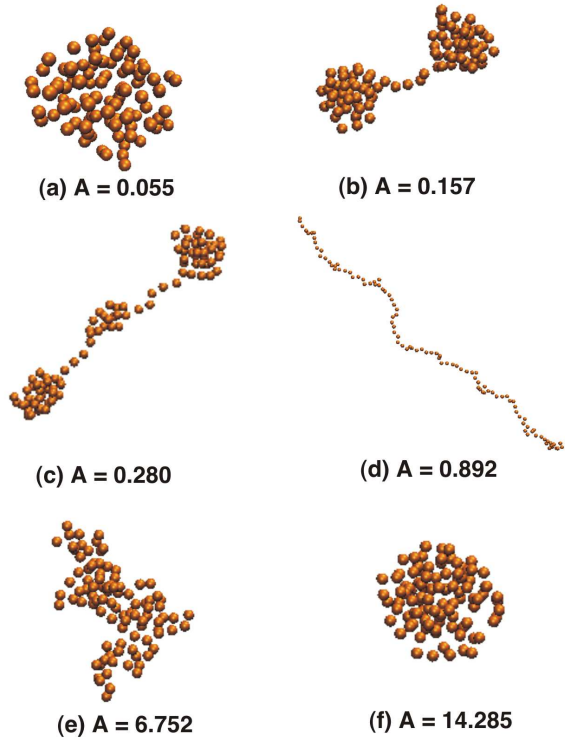


FIG. 1: Snapshots of the polyelectrolyte chain configurations for different values of  $A$ . For the sake of clarity, counterions are not shown and figures are not in the same scale. (a) Globular phase, (b) Dumbbell phase, (c) Pearl-necklace phase, (d) Extended phase, (e) Sausage phase and (f) Globular phase.

## B. Distribution of counterions

We consider a counterion to be condensed if its distance from any monomer is less than  $2\ell_B$  [12]. Let  $N_c$  be the number of condensed counterions and  $N$  the number of monomers. The mean fraction of condensed counterions  $\langle N_c/N \rangle$  as a function of  $A$  is shown in Fig. 2 for different  $N$ . With the above definition of a condensed counterion, it is observed that the counterion condensation starts slightly below  $A = 1$ , consistent with the findings in Ref. [36]. Note that for the case of an infinitely long and uniformly charged cylinder, the classic Manning condensation occurs at  $A = 1$ .

For a given value of  $A$ , the fraction of condensed counterions increases with increasing  $N$  and reaches a limiting value. A similar result was obtained for the good solvent case as well [12]. The dependence of the fraction of condensed counterions on  $N$  is closely linked to the effective size or morphology of the polyelectrolyte chain. We show that the longer chains have smaller relative size for values of  $A$  at which the counterion condensation occurs. The dependence of the relative size of the chain on  $N$  can be studied by calculating the radius of gyration  $R_g$ , defined

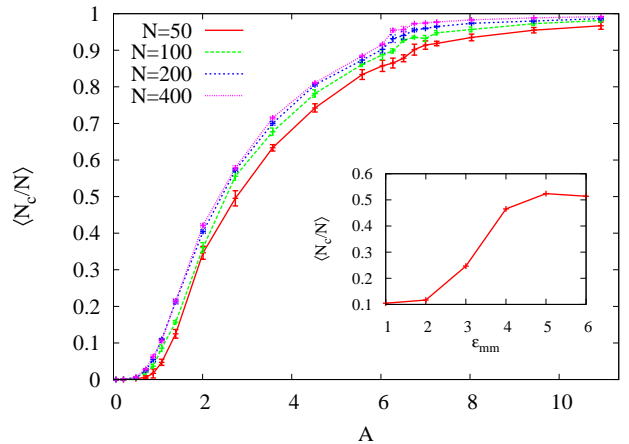


FIG. 2: Mean fraction of counterions  $\langle N_c/N \rangle$  within a distance  $2\ell_B$  from the polyelectrolyte chain as a function of  $A$ . Inset:  $\langle N_c/N \rangle$  as a function of the monomer-monomer attraction energy  $\epsilon_{mm}$  for  $N = 100$  and  $A = 0.89$ .

as

$$R_g = \sqrt{\frac{1}{N} \sum_{i=1}^N (\vec{r}_i - \vec{r}_{cm})^2}, \quad (6)$$

where  $\vec{r}_i$  is the position of the  $i^{th}$  particle and  $\vec{r}_{cm}$  is the centre of mass of the chain. For fixed  $A$ ,  $R_g/N$ , a measure of the relative extension, decreases with  $N$  in the region  $A \gtrsim 0.89$  where the condensation occurs (see Fig. 3).

These two observations, the effective size being smaller for larger chains, and longer chains having a larger fraction of condensed counterions (see Fig. 2), are related. We argue that a polymer with a smaller effective size has more condensed counterions. In the inset of Fig. 2, we show that increasing  $\epsilon_{mm}$  (depth of the Lennard-Jones potential of monomer-monomer pairs), keeping other parameters fixed, results in increased condensation. It is clear that increasing  $\epsilon_{mm}$  can only result in the effective size of the polyelectrolyte chain becoming smaller. The increased condensation may be due to counterions experiencing lower electrostatic potential for a more compact chain.

We also observe that  $R_g/N$  shows a jump around  $A_c \approx 6.25$ . The jump is more pronounced for longer chains. For  $A > 6.25$ , radius of gyration  $R_g$  scales as  $N^{1/3}$ , indicating that the chain is in a collapsed phase. We also observe a small kink in the fraction of condensed ions (see Fig. 3) around the same value of  $A$  where  $R_g/N$  shows a jump.

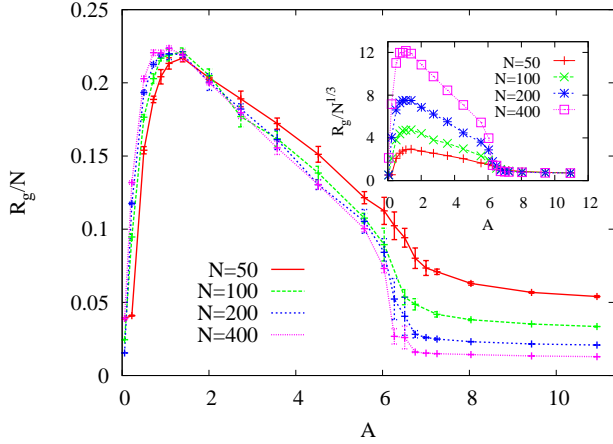


FIG. 3: Ratio of the radius of gyration  $R_g$  to the number of monomers  $N$  as a function of  $A$ . Inset: The data for  $R_g/N^{1/3}$  collapse for different  $N$  for  $A \gtrsim 6.25$ .

### C. Number of non-bonded neighbours and the condensation transition

The number of non-bonded nearest neighbours of a monomer is a useful order parameter in studying the collapse transition of a neutral polymer [37]. We study its behaviour for the polyelectrolyte chain. For a given monomer, a non-bonded neighbour is defined as any monomer/counterion that is not connected to it by a bond and within a distance  $b$ . The variation of the mean number of non bonded neighbours per monomer  $\langle n_b \rangle$  with  $A$  is shown in Fig. 4.  $\langle n_b \rangle$  decreases when the polyelectrolyte chain goes from the initial collapsed phase to the extended phase. It has the minimum around  $A' \approx 0.89$  where the chain is most extended. Close to  $A_c \approx 6.25$ ,  $\langle n_b \rangle$  has a jump with the jump size increasing with number of monomers  $N$ . This value of  $A$  corresponds to the collapse transition of the condensed polyelectrolyte (see inset of Fig. 3).

We also study the relative fluctuations  $\chi_b$  of the number of non-bonded neighbours, where

$$\chi_b = \frac{N [\langle n_b^2 \rangle - \langle n_b \rangle^2]}{\langle n_b \rangle^2}. \quad (7)$$

It has a peak around  $A' \approx 0.89$  (see Fig. 5). The increasing peak height with the number of monomers  $N$ , indicates a divergence in the thermodynamic limit. This critical value  $A'$  corresponds to the onset of condensation of the counterions. At this value of  $A$ , the polyelectrolyte chain is fully extended and hence this condensation is reminiscent of Manning condensation. The data for different values of  $N$  can be collapsed using the scaling form

$$\chi_b \approx N^{\phi_1} f [(A - A')N^{\phi_2}], \quad N \gg 1, \quad (8)$$

where  $\phi_1$  and  $\phi_2$  are scaling exponents. Data collapse is seen for  $\phi_1 \approx 0.20$  and  $\phi_2 \approx 0.15$  (see inset of Fig. 5).

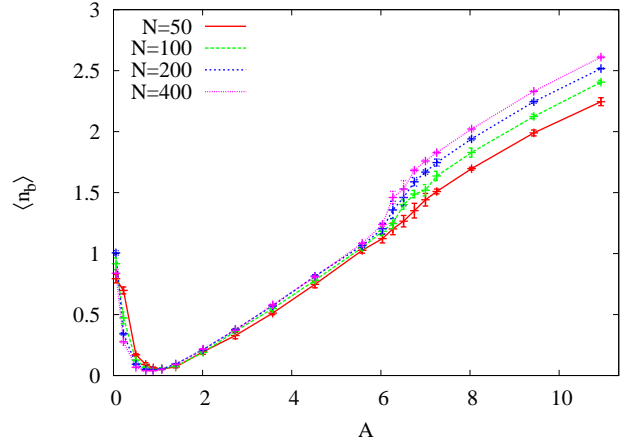


FIG. 4: The number of non bonded neighbours per monomer  $\langle n_b \rangle$  as a function of  $A$  for different  $N$

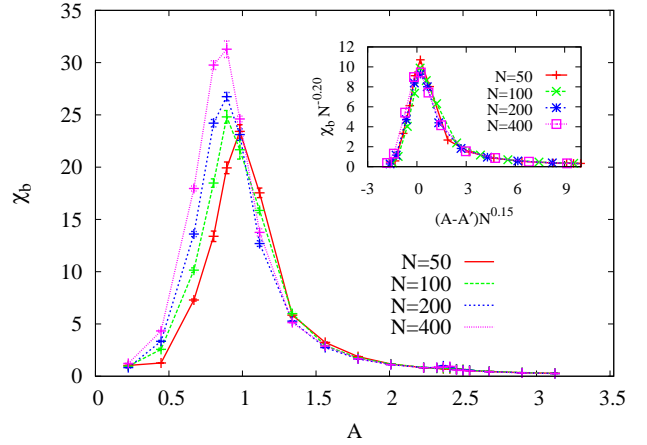


FIG. 5: The relative fluctuation  $\chi_b$  of the number of non bonded neighbours, as defined in Eq. (7), as a function of  $A$  for different  $N$ . Inset: Data collapse when  $\chi_b$  and  $A$  are scaled as in Eq. (8), where  $A' = 1.08$  for  $N = 50$  and  $A' = 0.89$  otherwise.

Divergence of  $\chi_b$  with data collapse is a strong indication of condensation being a continuous phase transition. Earlier discussion of the order of the Manning like condensation has been restricted only to model systems of cylinder in three dimensions and disc in two dimensions, and a similar continuous transition has been reported in such systems [26–28].

### D. Transition from extended phase to collapsed phase

To quantify the transition from the extended phase to the collapsed phase, the electrostatic energy per monomer  $E_c$  and its fluctuations are calculated. Only monomer-monomer pairs are used for calculating these quantities since we are interested in the configuration of

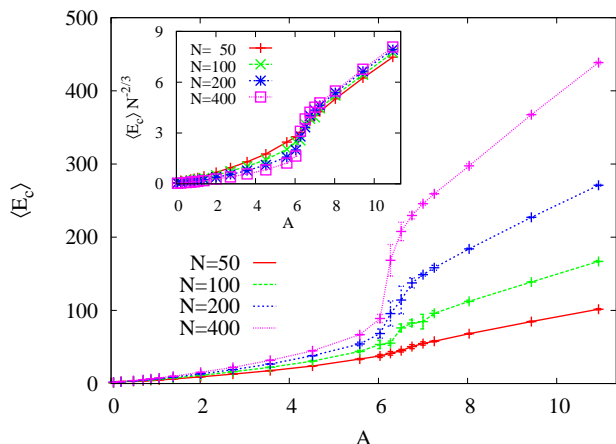


FIG. 6: Mean Coulomb energy per monomer  $\langle E_c \rangle$  as a function of  $A$  for different  $N$ . Inset:  $\langle E_c \rangle \sim N^{2/3}$  in the collapsed phase.

the polyelectrolyte chain. The relative fluctuation  $\chi_c$  in the electrostatic energy is defined as

$$\chi_c = \frac{N [\langle E_c^2 \rangle - \langle E_c \rangle^2]}{\langle E_c \rangle^2}. \quad (9)$$

The mean electrostatic energy per monomer  $\langle E_c \rangle$  increases with  $A$  and has an abrupt jump at  $A_c \approx 6.25$  (see Fig. 6). The jump is more pronounced for higher values of  $N$ . In the collapsed phase, the shape of the chain is roughly spherical and hence  $\langle E_c \rangle$  should scale as  $N^{2/3}$  [38]. For  $A > A_c$ , we confirm that  $\langle E_c \rangle$  scales as  $N^{2/3}$  (see inset of Fig. 6). The scaling of  $\langle E_c \rangle$  as  $N^{2/3}$  along with the scaling of  $R_g$  as  $N^{1/3}$  (see inset of Fig. 3) in this regime confirm that the polymer is indeed in a collapsed configuration.

The variation of the relative fluctuation  $\chi_c$  with  $A$  is shown in Fig. 7.  $\chi_c$  has a peak at  $A_c$ , close to the value of  $A$  at which  $\langle E_c \rangle$  has a discontinuity. The peaks are not resolved to the desired accuracy. This is because, close to the transition point, the polyelectrolyte chain fluctuates between the extended and the collapsed phases during the time evolution. The inset of Fig. 7 shows a sample time series of  $E_c$ , near the transition point, for  $N = 200$ , where  $E_c$  fluctuates roughly between two values. This behaviour of  $\chi_c$  coupled with the sharp rise in  $\langle E_c \rangle$  (see Fig. 6) suggests a first order phase transition. Our findings are consistent with the previous theoretical results [39] that the extended to collapse transition of a polyelectrolyte chain is first order.

Similar divergence in the fluctuation of the electrostatic energy per monomer has been observed for the transition of a polyelectrolyte chain, in a poor solvent, from the initial globular phase to the dumbbell and trimbell phases in the absence of explicit counterions [7].

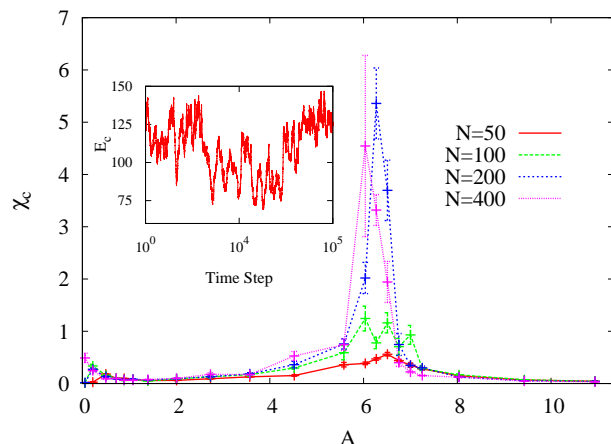


FIG. 7: Fluctuation in the Coulomb energy per monomer  $\chi_c$  as a function of  $A$ . Inset: Time series of the electrostatic energy per monomer, for  $N = 200$ , and  $A = 6.50$ .

### E. Existence of Sausage phase

The sausage phase was defined in Ref. [15] as a collapsed phase where mean asphericity is non-zero. We show below that the transition associated with change in asphericity coincides with the collapse transition. We define asphericity  $Y$  as

$$Y = \left\langle \frac{\lambda_1 - \frac{\lambda_2 + \lambda_3}{2}}{\lambda_1 + \lambda_2 + \lambda_3} \right\rangle, \quad (10)$$

where  $\lambda_{1,2,3}$  are the eigenvalues of the moment of inertia tensor with  $\lambda_1$  being the largest eigenvalue. The moment of inertia tensor  $G$  is

$$G_{\alpha\beta} = \frac{1}{N} \sum_{i=1}^N r_{i\alpha} r_{i\beta}, \quad (11)$$

where  $r_{i\alpha}$  is the  $\alpha^{th}$  component of the position vector  $\vec{r}_i$ . Asphericity  $Y$  is zero for a sphere (collapsed globule) and one for a linear rod (extended configuration). For all other configurations, it has a value between zero and one.

The variation of asphericity with  $A$  for different  $N$  is shown in Fig. 8. For very small values of  $A$ , asphericity increases corresponding to the extension of the initial collapsed phase. In the extended region  $0.89 \lesssim A \lesssim 6.25$ , asphericity increases with  $N$  and tends to one for large  $N$ . For  $A \gtrsim 6.25$ , asphericity decreases to zero with  $N$  as a power law (see inset of Fig. 8). Thus, for large  $N$ , asphericity jumps from one to zero as  $A$  crosses  $A_c \approx 6.25$ . The value of the transition point coincides with the extended to collapsed transition discussed in Sec. III D. As there is no second transition in asphericity or in  $\langle E_c \rangle$ , we conclude that the sausage phase suggested in Ref. [15] is identical with the collapsed phase and is not a different phase.

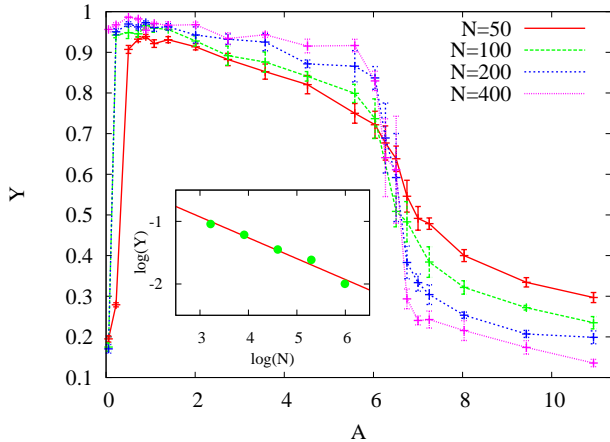


FIG. 8: Asphericity  $Y$  (as defined in Eq. (10)) as a function of  $A$ . Inset: Variation of asphericity  $Y$  with chain length  $N$  for  $A = 10.93$ . The slope of the straight line is  $-0.33$ .

#### IV. CONCLUSIONS

Using molecular dynamics simulations, we studied the phase diagram and phase transitions between the phases of a single polyelectrolyte chain in a poor solvent. The counterions were taken care of explicitly while the solvent was implicit. The dependence of various physical quantities on  $A$ , a dimensionless number that parametrised the strength of the electrostatic interaction, were calculated for different chain lengths  $N$ . Our main results are summarised below.

We quantified the transition associated with the condensation of counterions on the extended chain. The fluctuations of the non-bonded neighbours  $\chi_b$  diverges

at  $A' \approx 0.89$  with exponents that indicate a continuous transition. While the value of the exponents we obtained are not accurate, they indicate that data for different system sizes can be explained by one scaling function. It would be interesting to study the number of non-bonded neighbours and its fluctuations for the good solvent problem as well as in the presence of salt.

We also analysed the sausage phase introduced in Ref. [15] as a new intermediate phase between the extended and collapsed phases. We show that the transition associated with the discontinuity in asphericity and that associated with the extended to collapsed transition occur, within numerical error, at the same value of  $A$  ( $A_c \approx 6.25$ ). This, in conjunction with the fact that there is no second transition for either quantity, strongly suggests that the sausage phase does not exist independent of the collapsed phase, and was probably an artefact of earlier simulations [15] of chains of small size.

The extended to collapsed transition of the condensed polymer chain was also quantified. The abrupt jump in  $R_g/N^{1/3}$ , in the mean electrostatic energy  $\langle E_c \rangle$ , and mean number of non-bonded nearest neighbours  $\langle n_b \rangle$ , transition of the chain between extended phase and collapsed phase near the transition point, combined with the peaks in the fluctuations of the electrostatic energy  $\chi_c$ , are evidences for a first order transition. This is consistent with the theoretical prediction in Ref. [39].

In addition, we find that the fraction of condensed counterions increases with  $N$  for fixed  $A$  in the extended phase. By studying its dependence on  $\epsilon_{mm}$  and the dependence of  $R_g/N$  on  $N$ , we argued that the increase in the fraction is related to longer chains having a smaller relative extension.

- 
- [1] A. V. Dobrynin and M. Rubinstein, *Prog. Polym. Sci* **30**, 1049 (2005).
- [2] Y. Levin, *Rep. Prog. Phys.* **65**, 1577 (2002).
- [3] R. R. Netz and D. Andelman, “Encyclopedia of electrochemistry,” (Wiley-VCH, 2002) p. 282.
- [4] Y. Kantor and M. Kardar, *Europhys. Lett* **27**, 643 (1994).
- [5] Y. Kantor and M. Kardar, *Phys. Rev. E* **51**, 1299 (1995).
- [6] A. V. Dobrynin, M. Rubinstein, and S. P. Obukhov, *Macromolecules* **29**, 2974 (1996).
- [7] A. V. Lyulin, B. Dunweg, O. V. Borisov, and A. A. Darinskii, *Macromolecules* **32**, 3264 (1999).
- [8] Q. Liao, A. V. Dobrynin, and M. Rubinstein, *Macromolecules* **39**, 1920 (2006).
- [9] G. S. Manning, *J. Chem. Phys* **51**, 924 (1969).
- [10] M. Muthukumar, *J. Chem. Phys* **120**, 9343 (2004).
- [11] H. Schiessel and P. Pincus, *Macromolecules* **31**, 7953 (1998).
- [12] R. G. Winkler, M. Gold, and P. Reineker, *Phys. Rev. Lett* **80**, 3731 (1998).
- [13] U. Micka, C. Holm, and K. Kremer, *Langmuir* **15**, 4033 (1999).
- [14] H. J. Limbach and C. Holm, *J. Phys. Chem. B* **107**, 8041 (2003).
- [15] K. Jayasree, P. Ranjith, M. Rao, and P. B. S. Kumar, *J. Chem. Phys* **130**, 094901 (2009).
- [16] V. O. Aseyev, S. I. Klenin, H. Tenhu, I. Grillo, and E. Geissler, *Macromolecule* **34**, 3706 (2001).
- [17] C. E. Williams and M. D. C. Tinoco, *Europhys. Lett* **52**, 284 (2000).
- [18] M. D. C. Tinoco, R. Ober, I. Dolbnya, W. Bras, and C. E. Williams, *J. Phys. Chem. B* **106**, 12165 (2002).
- [19] M. N. Spiteri, C. E. Williams, and F. Boue, *Macromolecules* **40**, 6679 (2007).
- [20] V. O. Aseyev, H. Tenhu, and S. I. Klenin, *Macromolecules* **32**, 1838 (1999).
- [21] F. Bordini, C. Cametti, T. Gili, S. Sennato, S. Zuzzi, S. Dou, and R. H. Colby, *Phys. Rev. E* **72**, 031806 (2005).
- [22] P. Loh, G. R. Deen, D. Vollmer, K. Fischer, M. Schmidt, A. Kundagrami, and M. Muthukumar, *Macromolecules* **41**, 9352 (2008).
- [23] L. Rayleigh, *Phil. Mag* **14**, 184 (1882).
- [24] M. Deserno, *Eur. Phys. J. E* **6**, 163 (2001).

- [25] R. Chang and A. Yethiraj, *J. Chem. Phys.* **118**, 14 (2003).
- [26] A. Naji and R. R. Netz, *Phys. Rev. Lett.* **95**, 185703 (2005).
- [27] A. Naji and R. R. Netz, *Phys. Rev. E* **73**, 056105 (2006).
- [28] Y. Burak and H. Orland, *Phys. Rev. E* **73**, 010501(R) (2006).
- [29] W. B. Russel, D. A. Saville, and W. R. Schowalter, *Colloidal Dispersions* (Cambridge University Press, Cambridge, 1989).
- [30] <http://lammps.sandia.gov>.
- [31] S. J. Plimpton, *J. Comp. Phys.* **117**, 1 (1995).
- [32] S. Nosé, *J. Chem. Phys.* **51**, 511 (1984).
- [33] W. G. Hoover, *Phys. Rev. A* **31**, 1695 (1985).
- [34] R. W. Hockney and J. W. Eastwood, *Computer Simulations Using Particles* (McGraw-Hill, New York, 1975).
- [35] H. Gould, J. Tobochnik and W. Christian, *An Introduction to Computer Simulation Methods: Applications to Physical Systems* (Addison Wesley, San Francisco, 2007).
- [36] S. Liu and M. Muthukumar, *J. Chem. Phys.* **116**, 9975 (2002).
- [37] C. Vanderzande, *Lattice Models of Polymers* (Cambridge University Press, Cambridge, 1999).
- [38] L. D. Landau and E. M. Lifshitz, *Classical Theory of Fields* (Butterworth-Heinemann, Oxford, 1975).
- [39] N. V. Brilliantov, D. V. Kuznetsov, and R. Klein, *Phys. Rev. Lett.* **81**, 1433 (1998).